Materials Research. 2020; 23(1): e20190512
DOI: https://doi.org/10.1590/1980-5373-MR-2019-0512

Thermal Analysis on the Milled $Al+B_2O_3+Si+WO_3$ System to Synthesize Al_2O_3-WxSiy-WxBy Powders

Afshin Amiri Moghaddam*[a], *Mahdi Kalantar*[a]

[a]*Yazd University, Yazd, Safaeih, Iran*

Received: September 11, 2019; Revised: February 24, 2020; Accepted: March 1, 2020.

Composites including silicide of tungsten and boride of tungsten intermetallic compound as reinforced agents in alumina matrix have a good mechanical properties in low and high temperature (high friction resistance, strength, resin stance to creep and relatively high thermal shock resistance), moreover, they have chemical neutral with a high corrosion resistance in a high corrosive and high temperature environment. The purpose of this study is to investigate thermal analysis, phase and microstructural evaluation during synthesis of above mentioned composite by combustion aluminothermic processing in three systems 1-$Al+Si+WO_3$, 2-$Al+B_2O_3+WO_3$ and 3-$Al+B_2O_3+Si+WO_3$. A Ball-milled starting material according to stoichiometric ratio was thermal analyzed (DTA-TGA) for each of above mentioned system. The XRD results never show any new phase during ball-milling even up to 10 hours. The forming of tungsten silicide (W_xSi_y) is in lower temperature in comparison with tungsten boride (W_xB_y) during the thermal analysis experiments. The presence of Si in the $Al+B_2O_3+WO_3$ system facilitates the formation of tungsten borides. The microstructural observations show a uniform and dense distribution of silicide and boride of tungsten in the alumina matrix. Silicide phases are small grain with spherical morphology whereas; the boride phases are coarser and relatively elongated with irregular morphology.

Keywords: *Aluminothermic combustion synthesize, $Al+B_2O_3+Si+WO_3$ system, Phase analysis, Thermal analysis, gravity analysis, Micro structure analysis.*

1. Introduction

Ceramic based composite in comparison with metals and alloys have special advantages including high thermo mechanical properties high reaction, high chemical stability, low density, and high resistance to oxidation. In this respect, they are prioritized in high temperature components and structures such as cutting tools and aerospace applications. Due to the low coefficient of expansion and the lack of phase transformations and relatively high thermal conductivity for tungsten based intermetallic compounds (especially borides and silicide); these materials have relatively high thermal shock resistance. As such, nowadays cermet and composite materials containing such compounds are used as parts or as protector coating layer on the surface of metals and alloys[1-5]. One of the most well-known ceramics is alumina, which has special mechanical and physical properties. The results of our studies show that if nitride, boride, carbide and silicide compounds as secondary phase (reinforced phase) are added to Al_2O_3 as the matrix phase, mechanical and physical properties are significantly increased[6-13]. Various methods have been used for synthesis of composite powders including 1-in situ synthesis (mechanical alloying, reaction sintering, combustion synthesis (CS), self-propagating high temperature synthesis (SHS), carbothermic reduction, sol-gel, vortex casting and…)[14-18] and 2-non in situ synthesis (powder metallurgy)[19,20].

Froyen and Feng produced Al-Al_2O_3-ZrB_2 cermet in Al-ZrO_2-B_2O_3 using hot press method, which results in a composite with a tensile strength about 300 MPa[21]. The composites of Al_2O_3-WSi_2, Al_2O_3-WB and WSi_2-Mullite were synthesized by SHS aluminothermic (SHS-AT) processing in Al-Si-WO_3, Al-WO_3-B_2O_3[22] and Al-SiO_2-WO_3-B_2O_3[23] systems and composite WB_2-Mullite in Al-SiO_2-WO_3-B_2O_3 system[23].

The advantages of the combustion synthesis (In-situ CS and SHS) in comparison with other methods are having more simplicity, non-complex equipment, short time (high speed of process), energy savings, high homogeneous and stronger bond of reinforcement-matrix. In this study, combustion synthesis method was used in aluminothermic system of $Al+Si+WO_3+B_2O_3$ for synthesizing powder composite including WSi_2, WB_2 and Al_2O_3. Thermal analysis experiments were carried out to study the physicochemical reactions that take place during combustion synthesis processing. X-rays analysis and electron microscopy observation were applied to identify the phase and microstructure of obtained composites powders.

2. Materials and Methods

Aluminum, silicon, born oxide and tungsten oxide powders were used with chemical formulations of Al, Si, B_2O_3 and WO_3 (Table 1). The mixture of raw materials based on the stoichiometric composition and according to

*mkalantar@yazd.ac.ir

Table 1. Important properties of raw materials.

Powder material	Particles size (μm)	Purity (%)	Melting temperature (°C)	Boiling Temperature (°C)	Standard heat formation ΔH^{o}_{298} (Kj.mol^{-1})	Molar mass (gr.mol^{-1})	Density (gr.cm^{-3})	Company
Al	200-300	99.9	660	2470	-	27	2.7	Aldrich
B_2O_3	300-400	99.9	450	1860	-1253.50	70	2.5	Merck
WO_3	400-500	99.9	1473	1700	-842.70	232	7.2	Merck
Si	200-300	99.9	1414	3265	-	28	2.3	Aldrich

Table 2. The composition of the weight percentages of the primary mixtures and result composite obtained based on stoichiometric calculations in different aluminothermic systems.

weight percentages of the primary mixtures					weight percentages of result composite obtained			
Si	WO_3	B_2O_3	Al	Primary mixtures	Composites obtained	WB_2	WSi_2	Al_2O_3
16.37	67.84	-	15.79	ASW	ASW	-	70.18	29.82
-	56.58	17.08	26.34	ABW	ABW	50.24	-	49.76
7.74	61.71	9.31	21.54	ABSW	ABSW	27.39	31.92	40.69

Table 3. Standard Card Number for XRD Analysis

Phase type	Standard card number
B_2O_3	(00-013-0570)
WO_3	(01-1465-072)
Al	(00-1180-001) (00-1386-043)
WSi_2	(00-0195-011) (00-1085-044)
W_5Si_3	(00-0261-016)
WB	(00-0738-035)
WB_2 or W_2B_5	(00-1386-043)
W_2B	(00-0990-025)
$Al_6Si_2O_{13}$	(00-15-0776)
W	(00-0806-04)
Al_2O_3	(01-1125-071) (00-0712-005) (00-1468-042) (01-1126-017)
$B(OH)_3$	(00-0199-030)
$Al_{18}B_4O_{33}$	(00-0003-032)
Si	(01-2108-077)

the reactions performed in different systems including ASW, ABW, ABSW (Table 2), were homogenized in satellite mill (PBM 210-Nano shot-Ar-300 rpm) for 10 hours with a ball weight ratio of alumina to a powder of 10 to 1.

In order to investigate the physic-chemical alterations and to determine the temperature range of stability for each of the oxide, boride and silicide phases, the mixture of ball-milled powders were analyzed by differential thermal (DTA) and thermal gravity analysis (TGA) with a heating rate of 20°C. min^{-1}, under the atmosphere of argon (STA 504, Bahr Gmb 11-Germany). HSC software was used for calculations and thermodynamic studies[24]. X-ray Diffraction (XRD) analysis (GNR-Explorer, copper anode, 40 kV, 30 mA, counting time 0.5 seconds, step size 0.02) were used to determine the phase composition and scanning electron microscope (SEM) observation used for microstructure studies (Mira 3- XMU). Phases in the XRD spectra have been identified using standard cards as shown in Table 3.

3. Results and Discussion

3.1 ASW system

According to Figures 1a and 1b, the results of the thermal analysis and its XRD for ASW system respectively formed the tungsten silicide (W_5Si_3 and WSi_2) along with the alumina phase[25,26]. The DTA diagram (Figure 1a) shows a generally positive slope indicating that the reaction of aluminothermic and the formation of tungsten silicide (Reaction 1 to 4 in Table 4) become more and more exothermic by the increase of the temperature. The exothermic rate is intensified after the melting of aluminum (Endothermic peak at 660 °C) in such a manner that it raises up to 1000 °C. Tungsten oxide reduction reaction by Al (Reaction 1) while having more negative free energy changes (Figure 2) is dominant. In such condition, reaction 4 (Table 4) is performed simultaneously and tungsten silicides are formed. It should be mentioned that in all temperature ranges, free energy changes of forming W_5Si_3 (Reaction 2) relative to WSi_2 is more negative so that exothermic peak is formed at 1100 °C in relation to W_5Si_3 and exothermic peak is formed at 1250 °C in relation to WSi_2 (Reaction 3). The XRD results in Figure 1b represent the dominant phase of WSi_2, which is in accordance with the stoichiometry composition of the ASW system (Table 2).

3.2 ABW system

Figures 3a and 3b show the results of the thermal analysis up to 1300 °C and its XRD for the ABW sample. As such, according to Figure 3b, the tungsten phase is the main phase. Indicating the range of temperature up to 1300 °C is not sufficient for the formation of tungsten borides (Reactions 6, 7, 8 in Figure 4). The WO_3 and B_2O_3 have been reduced by Al up to 1200 °C (Reaction 1, 5 in Figure 4). Therefore, it is necessary to carry out heat treatment at higher temperatures to form tungsten boride. It should be noted that the non-appearance of boron and boron oxide in the range of XRD products can be due to their amorphous forms. The presence of the exothermic peak at 1000 °C in DTA curve (Figure 3a) belongs to aluminothermic reaction of WO_3 reduction and the exothermic peak at

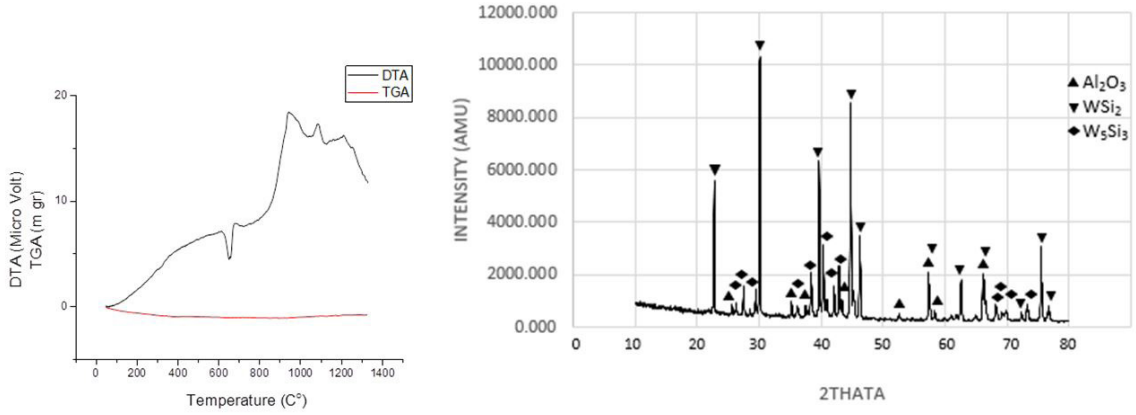

Figure 1. ASW system a) DTA-TGA with heating rate of 20 °C.min^{-1} and atmosphere of argon, b) XRD analysis of thermal analyzed sample.

Table 4. Thermodynamic information of reactions.

Number	Reaction	ΔG^o_{1273K} (kJ.mol^{-1})	ΔG^o_{1573K} (kJ.mol^{-1})	ΔG^o_{1773K} (kJ.mol^{-1})	ΔG^o_{1973K} (kJ.mol^{-1})	ΔG^o_T (kJ.mol^{-1})
1	$2Al+WO_3=Al_2O_3+W$	-750.668	-723.022	-703.180	-675.641	-850.200+0.089T
2	$5W+3Si=W_5Si_3$	-169.891	-178.229	-176.042	-164.085	-231.180+0.051T
3	$W+2Si=WSi_2$	-83.999	-81.465	-74.447	-60.783	-151.060+0.057T
4	$12Al+6WO_3+5Si= W_5Si_3+ WSi_2+ 6Al_2O_3$	-4.757.900	-4.597.825	-4.469.572	-4.278.712	-5483.400+0.642T
5	$2Al+B_2O_3=Al_2O_3+2B$	-310.093	-274.171	-250.105	-226.060	-354.370+0.047T
6	$2W+B=W_2B$	-75.651	-77.556	-78.662	-79.631	-75.977-0.001T
7	$W+B=WB$	-72.307	-74.035	-75.106	-76.105	-75.422+0.002T
8	$W+2B=WB_2$	-35.996	-36.596	-36.996	-37.396	-33.450-0.002T
9	$10Al+4WO_3+B_2O_3=5Al_2O_3+2WB+ WB_2$	-2.682.385	-2.579.185	-2.510.385	-2.441.585	-3120.297+0.344T
10	$1.5\ Si+WO_3=1.5\ SiO_2+W$	-504.937	-499.372	-490.243	-468.367	-603.820+0.085T
11	$1.5Si+B_2O_3=1.5SiO_2+2B$	-64.362	-50.522	-37.168	-18.786	-107.990+0.043T
12	$3Al_2O_3+2SiO_2=Al_6Si_2O_{13}$	-7.170.875	-7.253.357	-7.308.375	-7.363.375	-6820.800-0.275T
13	$28Al+12WO_3+6B_2O_3+12Si=5Al_2O_3 +3Al_6Si_2O_{13}+3WSi_2+6WB+3WB_2$	-10.288.182	-9.850.182	-9.558.182	-9.266.182	-12146.762+1.460T
14	$B(OH)_3 = HBO_2 + H_2O$	-	-	-	-	177.119-0.044T
15	$2HBO_2 = B_2O_3 + H_2O$	-	-	-	-	61.108-0.035T

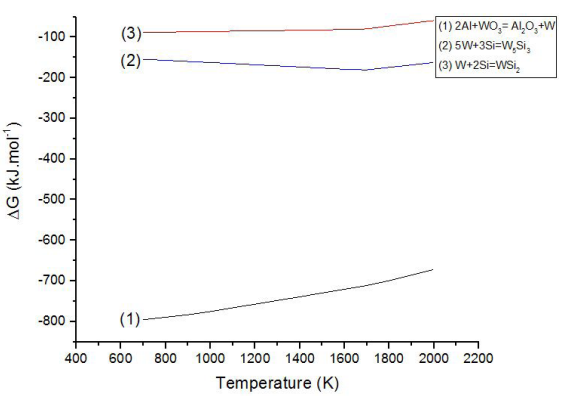

Figure 2. Free energy changes of reactions in ASW triple system as a function of temperature.

1200 °C belongs to simultaneous reduction of WO_3 and B_2O_3 (Reactions 1, 5 and strictly 9). It should be noted that thermodynamics only predicts the probability of reactions, but there is no debate about the kinetics of reactions. Investigations have shown that the kinetics of reactions in binary system of B-W (Rate of reaction – time), is S-shaped, that indicates the dependence of reactions on the atoms diffusion at a specified temperature[27]. Therefore, the heat treatment up to 1300 °C at a heating rate of 20 °C.min^{-1} has not been able to process the conditions for the formation of tungsten borides, and only formed a very small part of the W_2B and WB phases indicating the low boron activity and the low diffusible for solid-state reactions, especially when WB_2 is forming (X_B=0.66). The spinel phase of $A_{18}B_4O_{33}$ ($9Al_2O_3.2B_2O_3$) in XRD spectra (Figure 3b) was formed by no reduction of B_2O_3 and Al_2O_3 (formed by aluminothermic reaction).

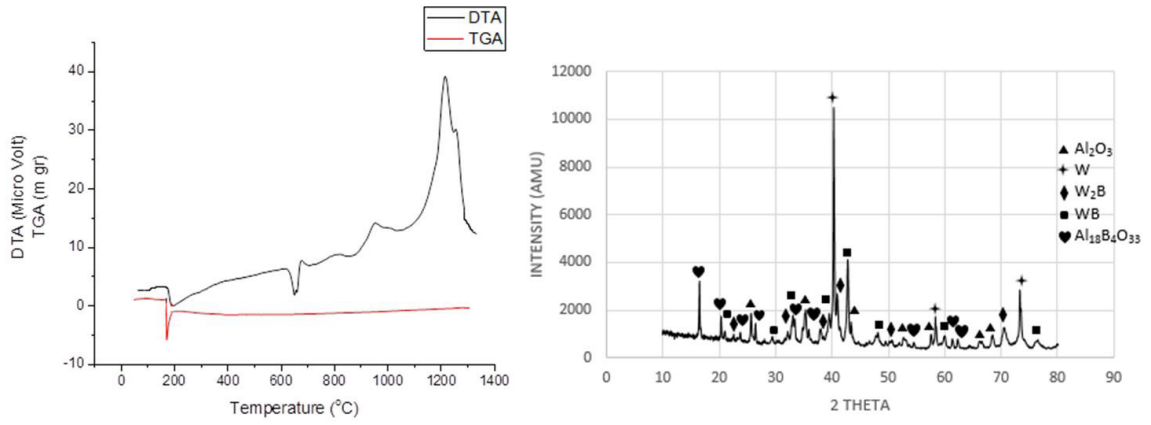

(a) (b)

Figure 3. ABW system a) DTA-TGA with heating rate of 20 °C.min^{-1} and atmosphere of argon, b) XRD analysis of thermal analyzed sample.

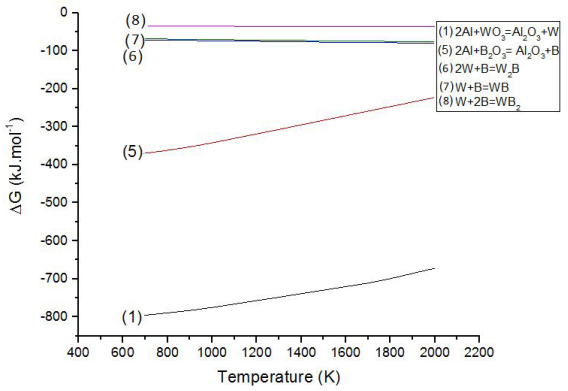

Figure 4. Free energy changes of reactions in ABW triple system as a function of temperature.

Demonstrative decreasing of the intensity of Al_2O_3 peak is according to Figure 3b. By performing re-testing of thermal analysis at temperature up to 1650 °C (Figures 5a and 5b), a peak at about 1650 °C (Figure 5a) is appeared that is related to forming of tungsten from boron and tungsten (Reactions 7, 8) according to Figure 5b. The XRD analysis in Figure 5b show complete removal of tungsten and the formation of tungsten borides. As a result, the role of increasing the temperature is important in improving the reactions between boron and tungsten elements. It must be marked that the middle phase of W_2B, (Appeared in Figure 3b) has completely changed into WB and WB_2 (W_2B_5) by increasing the temperature (W_2B+B=WB, WB+B=WB_2).

A small endothermic peak in 200 °C in the DTA curve and corresponded weight loss in TG curve (Figures 3a and 5a) is related to removing of molecular water and the decomposition of $B(OH)_3$ into B_2O_3. It should be noted that $B(OH)_3$ decomposes to B_2O_3 during two stays (Reactions of 14 and 15 in Table 4) at temperatures lower than 400 °C[28]. The $B(OH)_3$ compound is formed during the ball-milling process of starting the mixture of materials for two systems ABW and ABSW (Figure 6).

3.3 ABSW system

The ABSW system was studied (Table 2) to simultaneously benefit the advantages of tungsten silicide and borides. According to the results of XRD, for only ball-milled ABSW sample up to 10 hours no specific peak was observed relating to aluminothermic reaction and only a very small amount of B_2O_3 has transformed into $B(OH)_3$ due to presence of the moisture. It can be concluded that higher activation energy (Mechanical and thermal) is required for the initiation of aluminothermic reactions.

Figure 7a shows the results of DTA-TGA analyses performed on the ball-milled ABSW sample is in agreement with the results of ASW and ABW systems. Taking into account the thermodynamic data of Table 4, Figure 8 and Figures 7a and b, reactions of 1, 4 and 10 (Simultaneously) and reactions of 3,5,9,11,13 (Simultaneously) and reactions of 7, 8 were take placed at temperature range up to 1000 °C, 1100-1400 °C, 1450 °C, 1700 °C respectively. Due to the occurrence of several peaks simultaneously at temperature range from 1100 to 1400 °C; a spread peak with high intensity is formed. The peak occurred at 1700 °C (Reaction 8) for the ABSW is significantly stronger than the ABW system that can be related to higher temperature in the ABSW system (1700 °C against 1650 °C: It should be noted that the maximum temperature available in the thermal analysis system is 1700 °C.) and presence of Si in the ABSW system. On the other hand, thermodynamic and kinetic conditions of boron reduction and the formation of tungsten borides will be easier in presence of Si in such a manner that the phase is not appeared in the ABSW system (Figure 7b). For the ABW system, even up to 1650 °C, the spinel phase at $A_{18}B_4O_{33}$ is still stable (Figure 5b). According to the DTA curve in Figure 7a while increasing the temperature, the DTA curve is steadily increased and this can be related to the intensification of alumino and silicothermic reactions. It should be noted that the formation of mullite in ABSW system can be due to the role of silicon in the reduction of tungsten oxide or boron oxide and the formation of SiO_2 (Reactions of 10 and 11) and its reaction with Al_2O_3 (Reaction 12),

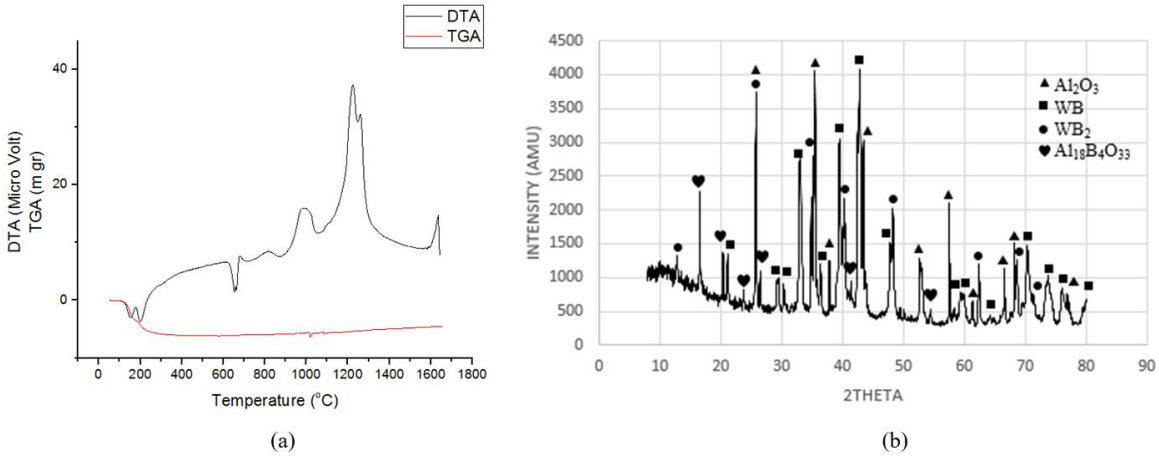

(a) (b)

Figure 5. ABW system a) DTA-TGA with rate of 20 °C.min^{-1} and atmosphere of argon, b) XRD analysis of thermal analyzed sample.

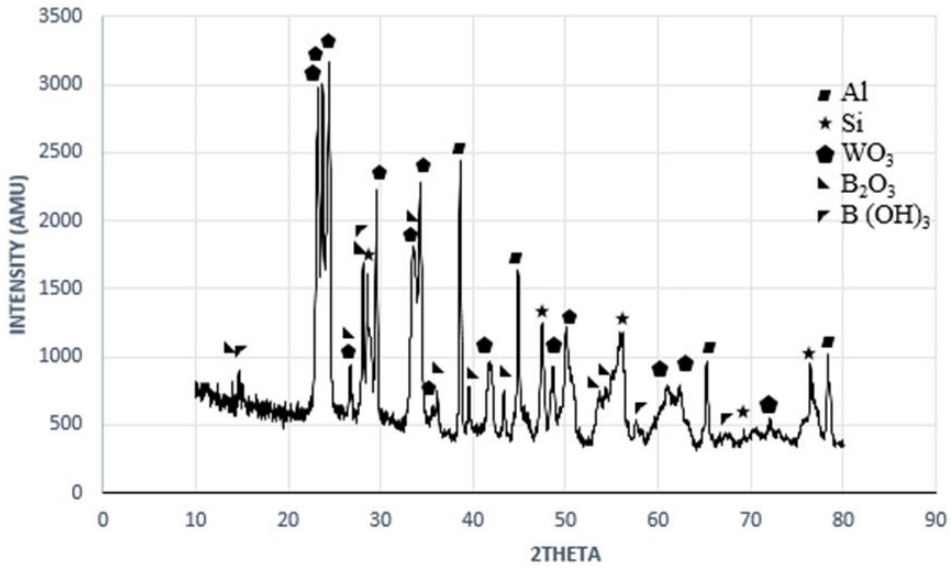

Figure 6. XRD analysis of the milled sample in the ABSW system for 10 hours.

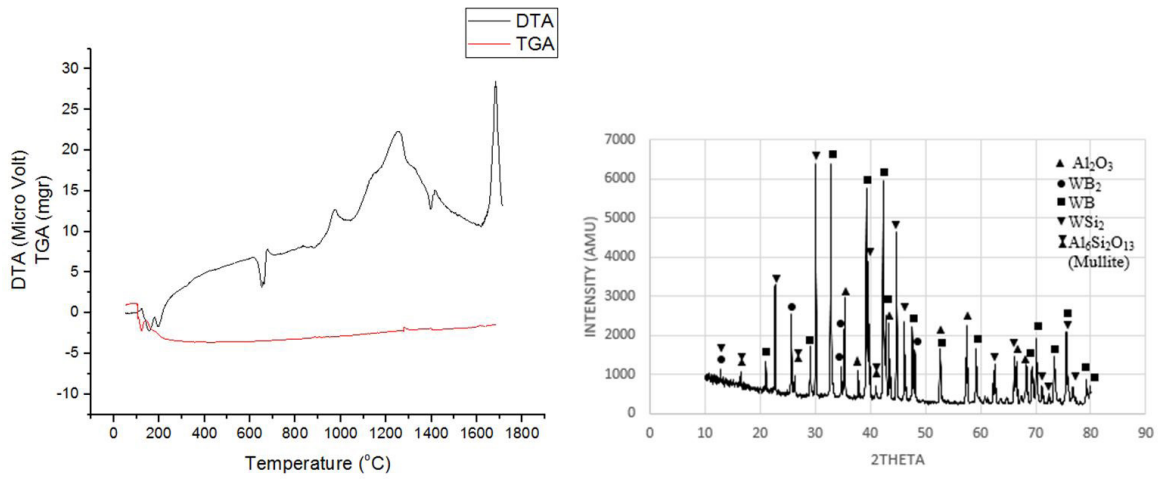

(a) (b)

Figure 7. ABSW system a) DTA-TGA with rate of 20 °C.min^{-1} and atmosphere of argon, b) XRD analysis of thermal analyzed sample.

The adiabatic temperature of combustion by using the given information in Tables 1 and 5 and the assumptions of non-melting components when considering the Equations 1 to 3 is calculated for three systems of ASW, ABW and ABSW. The result is given in Table 6. For the all three systems, according to merzanov criterion[29,30], self-propagating high temperature synthesis is occurred (T_{ad}>1800 k).

$$\Delta H°_{298} = (\Delta H°_{WB2} + \Delta H°_{WSi2} + 3\Delta H°_{Al2O3}) - (2\Delta H°_{WO3} + \Delta H°_{B2O3}) \quad (1)$$

$$\Delta H°_{298} \int_{298}^{T_{ad}} C_P^S = {}_{B2} \int_{298}^{T_{ad}} C_P^S + {}_{i2} + 3\int_{298}^{T_{ad}} C_{P12O3}^S \quad (2)$$

$$438.04T + 0.034T^2 + 10730000T^{-1} = 2387963.04 \quad (3)$$

Respectively according to Figures 9 and 10 SEM images and EDS analysis of the ABSW samples (Table 7), there is a uniform and dense distribution of reinforcing phases (Borides and silicide of tungsten) in the alumina matrixes. Silicide phase is the small grain with spherical morphology (Point A) whereas; the borides phase is more coursing and relatively elongated (Point B). The alumina phase is appeared as the coaxial grains with hexagonal morphology. Needle-shaped blades (D-points) are related to the mullite phase. The measurements of fine silicide grains size on FE-SEM images show an average of 200 nm (Figure 11a). Figures 11b and 11c show the hexagonal state of borides crystals obviously.

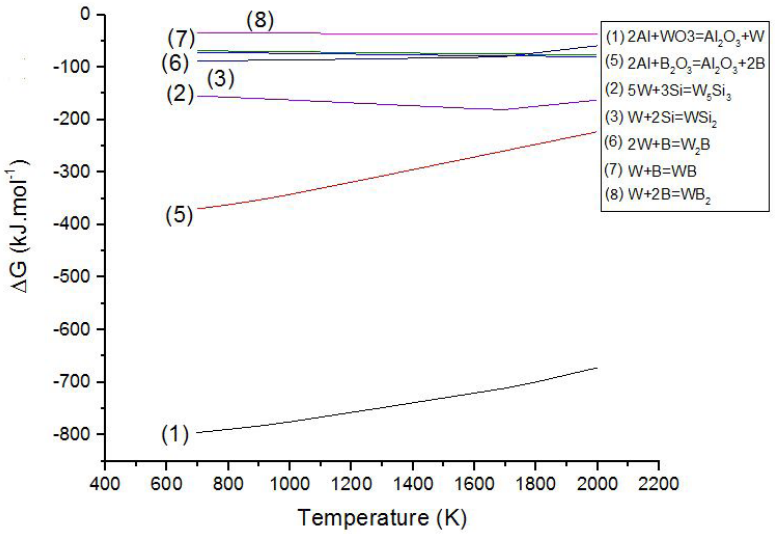

Figure 8. Free energy changes of reactions in ABSW triple system as a function of temperature.

Table 5. Thermodynamic information related to the calculation of the adiabatic temperature of the combustion front.

Composition	Standard formation enthalpy $\Delta H°_{298}$ (kJ.mol^{-1})	Solid state specific heat C^S_P J. (mol.K)$^{-1}$
WB_2	-33.50	50.42+0.003T–1569000T^{-2}
WSi_2	-92.90	67.82+0.011T–611000T^{-2}
Al_2O_3	-1676.90	106.6+0.017T –2850000T^{-2}

Table 6. Adiabatic temperature of different systems.

Adiabatic Temperature	Stoichiometric	Mixture
4240	$2Al+2Si+WO_3$	ASW
4070	$4Al+WO_3+B_2O_3$	ABW
4125	$6Al+2Si+2WO_3+B_2O_3$	ABSW

Table 7. EDS analysis for points A, B, C and D in Figure 10.

Related phases	Stoichiometry atomic percentage	Atomic percentage	Specified point
silicide tungsten	WSi_2: 67 Si, 33 W	49.95 Si, 53.05 W	A
	W_5Si_3: 37.5 Si, 62.5 W		
tungsten boride	WB: 50 B, 50 W	83.51 B, 16.49 W	B
	WB_2: 67 B, 33 W		
Alumina	60 O, 40 Al	58.21 O, 41.79 Al	C
Mullite	62 O, 9.5 Si, 28.5 Al	71.66 O, 21.28 Al and 7.06 Si	D

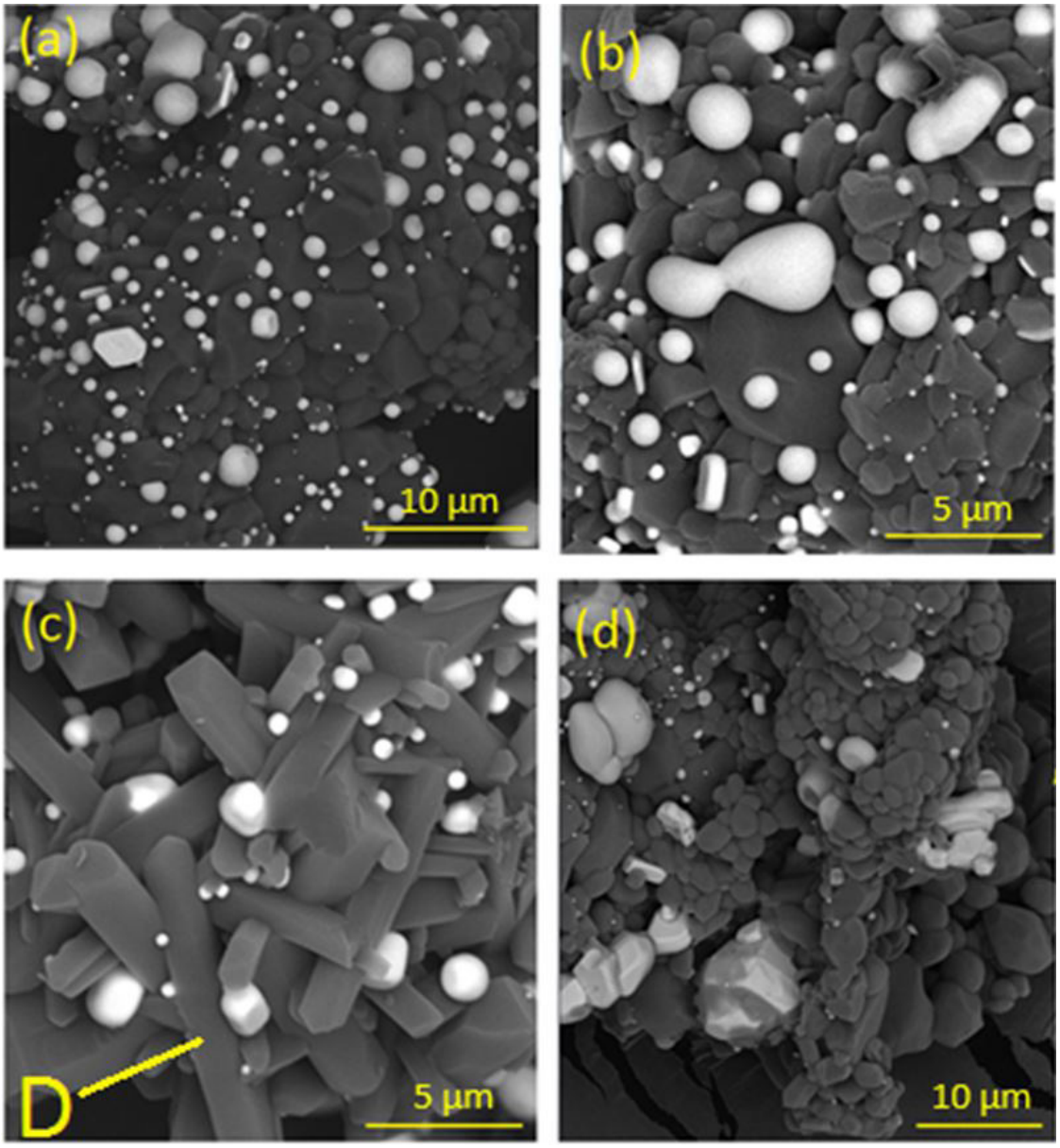

Figure 9. SEM images of the microstructure of different parts of the composite produced during the heat treatment at 1700 °C and the heating rate 20 °C.min^{-1} under argon atmosphere in ABSW system.

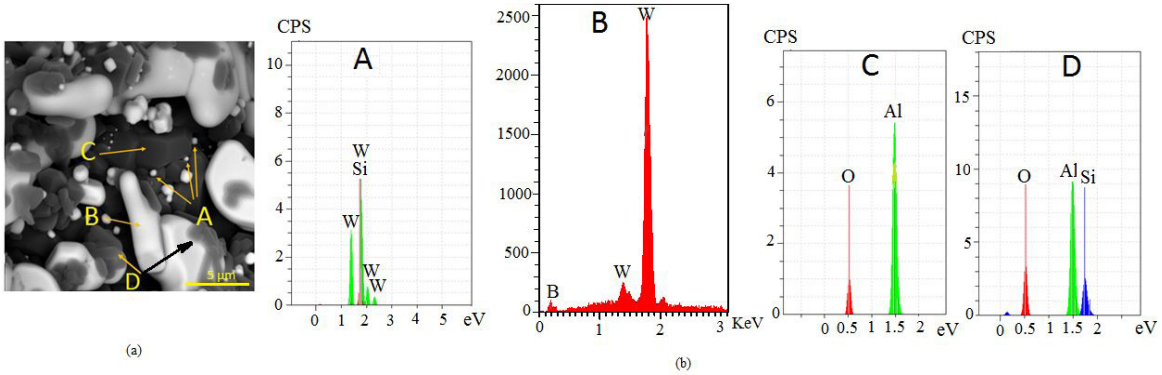

Figure 10. (a) SEM image and (b) EDS images of a heated sample at 1700 °C and a heating rate of 20 °C.min^{-1} under argon atmosphere in ABSW system, A: tungsten silicide, B: tungsten boride, C: Alumina, D: Mullite.

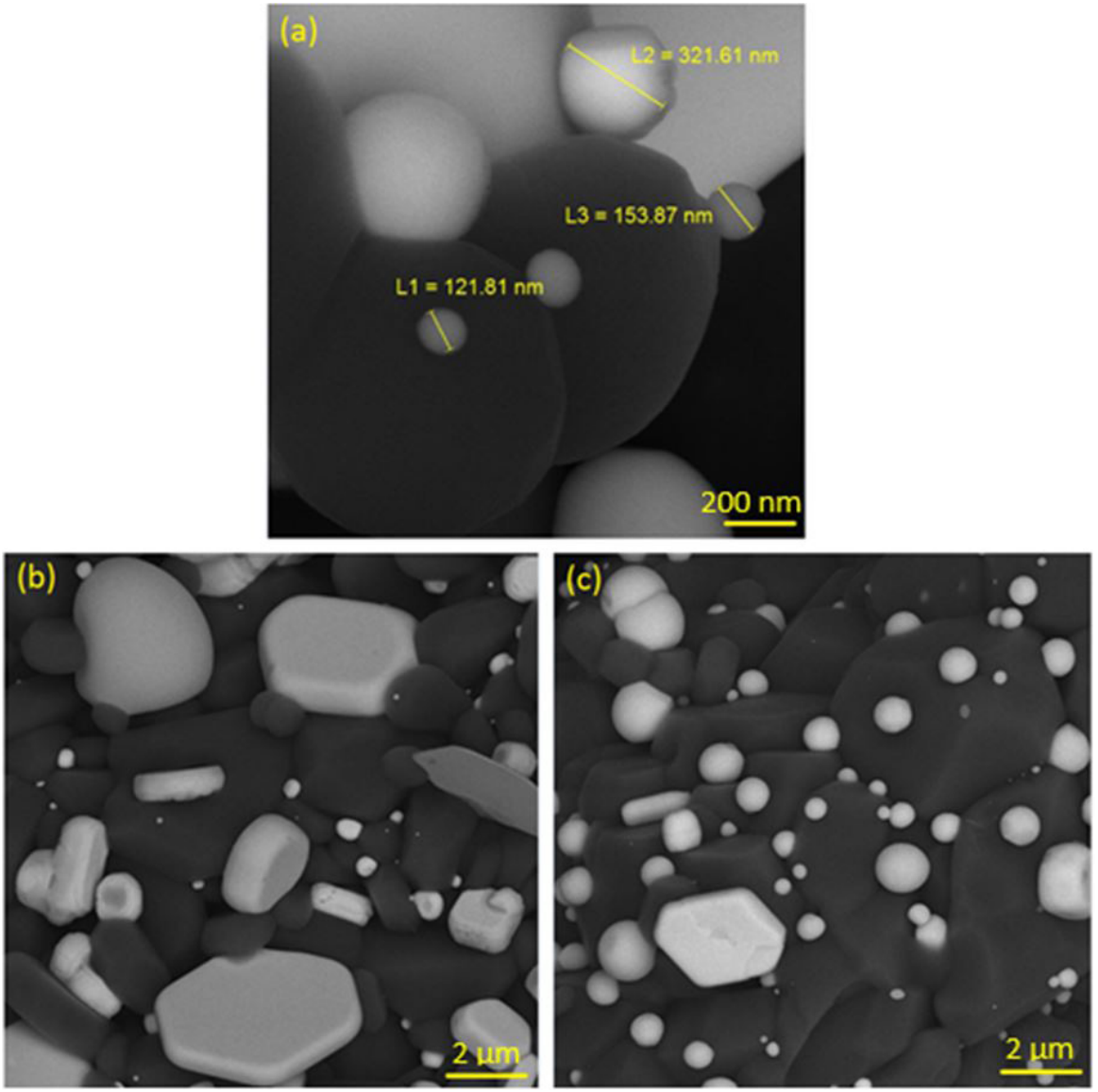

Figure 11. FE-SEM image of composite produced during heat treatment at 1700 °C and heating rate 20 °C.min^{-1} under argon atmosphere in ABSW system.

4. Conclusions

The obtained composite powder by combustion synthesis process in Al-B_2O_3-Si-WO_3- system shows a uniformly distribution of different phases of WSi_2, WB, WB_2 (Coarse grain with hexagonal morphology), mullite (Acicular grains) and Al_2O_3 (Hexagonal morphology). By the ball-milling process up to 10 hours for mentioned system, no new phase is observed and mechanical activation is only occurred. Results of thermodynamical studies show that, the combustion processing for all three systems of Al-B_2O_3-WO_3, Al-Si-WO_3 and Al-B_2O_3-Si-WO_3 is self-combustion process (Calculated T_{ad} is higher than 4000K). The tungsten silicide is formed at temperature ranges of 1000-1050 °C and 1200-1300 °C in the aluminothermic systems of Al-Si-WO_3 and Al-B_2O_3-Si-WO_3 respectively. While, the Carbide based compounds (WB and WB_2) are formed at temperature ranges of 1100-1400 °C and 1600-1700 °C in the aluminothermic systems of Al-B_2O_3-WO_3 and Al-B_2O_3-Si-WO_3 respectively. It is necessary to mention by the presence of Si in the Al-B_2O_3-Si-WO_3 system the formation of WB_2 is promoted.

5. References

1. Kalantar M. Structural high-temperature ceramics. 1st ed. Iran: Yazd University; 2009. 456 p.
2. Kalantar M. Composite materials based on ceramics (manufacturing, properties and usage. 1st ed. Iran: Yazd University; 2016. 1096 p.
3. Nihara K. New design concept of structural ceramics. J Ceram Soc. 1991;99(1154):974-82. http://dx.doi.org/10.2109/jcersj.99.974.
4. Jones R. Mechanics of composite materials. 2nd ed. Blacksburg, Virginia: Butterworths; 1999. 270 p.
5. Mishra SK, Gokuul V, Paswan S. Alumina-titanium diboride in situ composite by self-propagating high-temperature synthesis

(SHS) dynamic compaction: effect of compaction pressure during synthesis. Materials. 2014;43(1):19-24.
6. Otani S, Ishizawa Y. Preparation of WB_{2-x} single crystals by the floating zone method. J Cryst Growth. 1995;154(1–2):81-4. http://dx.doi.org/10.1016/0022-0248(95)00155-7.
7. Mohammadi R, Lech AT, Xie M, Weaver BE, Yeung MT, Tolbert SH, et al. Tungsten tetra boride, an inexpensive super hard material. Proc Natl Acad Sci USA. 2011;108(27):10958-62. http://dx.doi.org/10.1073/pnas.1102636108. PMid:21690363.
8. Yeh CL, Peng JA. Fabrication of WSi_2-Al_2O_3 and W_5Si_3-Al_2O_3 composites by combustion synthesis involving thermite reduction. Ceram Int. 2016;42(12):14006-10. http://dx.doi.org/10.1016/j.ceramint.2016.06.006.
9. Meschter PJ, Schwartz DS. Silicide-matrix materials for high temperature applications. J Miner Met Mater Soc. 1989;41(11):52-5. http://dx.doi.org/10.1007/BF03220384.
10. Petrovic JJ, Vasudevan AK. Key developments in high temperature structural silicides. Mater Sci Eng A. 1999;261(1-2):1-5. http://dx.doi.org/10.1016/S0921-5093(98)01043-0.
11. Peters ST. Handbook of composites. 2nd ed. California: Chapman & Hall; 1998. 1069 p. http://dx.doi.org/10.1007/978-1-4615-6389-1.
12. Valery V, Evgeny M. Mechanics and analysis of composite materials. 1st ed. USA: Elsevier Science; 2001. 424 p.
13. Zmii VI, Patokin AP, Khrebtov VL, Shirokov BM. Molybdenum-based oxidation-resistant $MoSi_2$–Al_2O_3 and WSi_2–Al_2O_3 coatings. Powder Metall Met Ceramics. 2008;47(11-12):693-7. http://dx.doi.org/10.1007/s11106-009-9080-4.
14. Lapin J, Štamborská M, Pelachová T, Bajana O. Fracture behavior of cast in-situ TiAl matrix composite reinforced with carbide particles. Mater Sci Eng A. 2018;721(1):1-7. http://dx.doi.org/10.1016/j.msea.2018.02.077.
15. Roghani H, Tayebifard SA, Kazemzadeh A, Nikzad L. Phase and morphology studies of B_4C-SiC nanocomposite powder synthesized by MASHS method in B_2O_3, Mg, C and Si system. Adv Powder Technol. 2015;26(4):1116-22. http://dx.doi.org/10.1016/j.apt.2015.05.007.
16. Farhadinia F, Sedghi A, Nooghani MT. properties of an Al/(Al_2O_3+TiB_2+ZrB_2) hybrid composite manufactured by powder metallurgy and hot pressing. J Appl Mech Tech Phys. 2017;58(3):454-60. http://dx.doi.org/10.1134/S0021894417030105.
17. Amiri-Moghaddam A, Kalantar M. In-situ synthesis of WC–X%Co composite in the WO_3–Co_3O_4–C system by carbothermal reduction method. J Aust Ceram Soc. 2017;53(2):839-45. http://dx.doi.org/10.1007/s41779-017-0097-8.
18. Rendtorff NM, Suárez G, Sakka Y, Aglietti EF. Dense mullite zirconia composites obtained from the reaction sintering of milled stoichiometric alumina zircon mixtures by SPS. Ceram Int. 2014;40(3):4461-70. http://dx.doi.org/10.1016/j.ceramint.2013.08.119.
19. Hasani S, Panjepour M, Shamanian M. A study of the effect of aluminum on $MoSi_2$ formation by self-propagation high-temperature synthesis. J Alloys Compd. 2010;502(1):80-6. http://dx.doi.org/10.1016/j.jallcom.2010.04.159.
20. Zhao Q, Shen Y, Ji M, Zhang L, Jiang T, Li C. Effect of carbon nanotube addition on friction coefficient of nanotubes/hydroxyapatite composites. J Ind Eng Chem. 2014;20(2):544-8. http://dx.doi.org/10.1016/j.jiec.2013.04.040.
21. Feng CF, Froyen L. In situ P/M Al/(ZrB_2+Al_2O_3) MMCs: processing, microstructure and mechanical characterization. Acta Mater. 1999;47(18):4571-83. http://dx.doi.org/10.1016/S1359-6454(99)00326-2.
22. Chanadee T, Wannasin J, Niyomwas S. Synthesis of WSi_2 and W_2B intermetallic compound by in-situ self-propagating high-temperature synthesis reaction. J Ceram Soc Jpn. 2014;122(6):496-501. http://dx.doi.org/10.2109/jcersj2.122.496.
23. Yeh CL, Kang CH. Formation of WB_2/mullite composites by reduction-based combustion synthesis with Al and Si as reductants and excess B_2O_3 addition. Ceram Int. 2017;43(13):9968-72. http://dx.doi.org/10.1016/j.ceramint.2017.05.008.
24. Outokumpu HSC. Chemistry® for windows, version HSC 4.1. Finland: Outokumpu Research Oy; 1999.
25. lı D, Ağaoğulları D, Öveçoğlu ML. Characterization of SiO_2-encapsulated WSi_2/W_5Si_3 nanoparticles synthesized by a mechanochemical route. Ceram Int. 2018;44(8):9442-53. http://dx.doi.org/10.1016/j.ceramint.2018.02.161.
26. Ovalı D, Ağaoğulları D, Öveçoğlu ML. Room-temperature synthesis of tungsten silicide powders using various initial systems. Int J Refract Met Hard Mater. 2019;82(1):58-68. http://dx.doi.org/10.1016/j.ijrmhm.2019.03.028.
27. Ghorbantabar Omran J, Sharifitabar M, Shafiee Afarani M. On the self-propagating high-temperature synthesisof tungsten boride containing composite powders from WO3–B2O3–Mg system. Ceram Int. 2018;44(12):14355-62. http://dx.doi.org/10.1016/j.ceramint.2018.05.044.
28. Sevim F, Demir F, Bilen M, Okur H. Kinetic analysis of thermal decomposition of boric acid from thermogravimetric data. Korean J Chem Eng. 2006;23(5):736-40. http://dx.doi.org/10.1007/BF02705920.
29. Merzhanov AG. combustion processes that synthesize materials. J Mater Process Technol. 1996;56(1-4):222-41. http://dx.doi.org/10.1016/0924-0136(95)01837-9.
30. Munir ZA, Anselmi-Tamburini U. Self-propagating high-temperature synthesis of hard materials. In: Riedel R, editor. Handbook of ceramic hard materials. 1st ed. Weinheim: John Wiley & Sons; 2000. p. 322-73. http://dx.doi.org/10.1002/9783527618217.ch11.